CHEMISTRY OF MATERIALS

Communication

pubs.acs.org/cm

First Principles Study of the $Li_{10}GeP_2S_{12}$ Lithium Super Ionic Conductor Material

Yifei Mo, Shyue Ping Ong, and Gerbrand Ceder*

Department of Materials Science and Engineering, Massachusetts Institute of Technology, Cambridge, Massachusetts 02139, United States

Supporting Information

KEYWORDS: *lithium ionic conductor, solid electrolyte, $Li_{10}GeP_2S_{12}$, ab initio, molecular dynamics, phase diagrams*

The continued drive for high performance lithium batteries has imposed stricter requirements on the electrolyte materials.[1,2] Solid electrolytes comprising lithium super ionic conductor materials exhibit good safety and stability and are promising to replace current organic liquid electrolytes. One major limitation in the application of Li-ion conductors is that their typical conductivity is less than 10^{-4} S/cm at room temperature. Recently, Kamaya et al. reported a new Li super ionic conductor $Li_{10}GeP_2S_{12}$ (LGPS), which has the highest conductivity ever achieved among solid lithium electrolytes of 12 mS/cm at room temperature (comparable conductivity with liquid electrolytes) and outstanding electrochemical performance in Li batteries.[3]

The high conductivity in LGPS is attributed to the fast diffusion of Li^+ in its crystal structural framework, which consists of $(Ge_{0.5}P_{0.5})S_4$ tetrahedra, PS_4 tetrahedra, LiS_6 octahedra, and LiS_4 tetrahedra. Kamaya et al. proposed that diffusion in LGPS occurs along one dimension (1D) with diffusion pathways along the *c* axis.[3] The authors also proposed that Li atoms in LiS_4 tetrahedra enable fast diffusion along the *c* direction, while Li atoms in LiS_6 octahedra are not active for diffusion. This hypothetical diffusion mechanism in LGPS has been inferred from the large anisotropic thermal factors and the Li disorder in the 1D channels but has not been directly proven. Understanding this LGPS material is important to improve its performance and may provide insight into designing new Li super ionic conductor materials.

Using first principles modeling, we investigated the diffusivity, stability, and electrochemical window of LGPS. We provide a hypothesis for the observed wide electrochemical window of LGPS. We also identified the diffusion pathways and calculated the corresponding activation energies and diffusion coefficient.

All calculations in this study were performed using the Vienna *Ab initio* Simulation Package (VASP)[4] within the projector augmented-wave approach.[5] Unless otherwise noted, all calculations were performed using the Perdew–Burke–Ernzerhof generalized-gradient approximation (GGA) to density functional theory (DFT).[6]

We assessed the phase stability of LGPS by constructing the quaternary Li–Ge–P–S phase diagram using all known Li–Ge–P–S compounds in the Inorganic Crystal Structure Database,[7] all $Li_xP_yS_z$ compounds compiled by Holzwarth et al.,[10] and the calculated ground state of LGPS. As the refined structure has partial occupancies, we ordered the arrangement of Li, Ge, and P atoms in LGPS using an electrostatic energy criterion.[8] Of the 10 orderings with the lowest electrostatic energy, the structure with the lowest calculated DFT energy was selected as the representative ground state. The calculation input parameters are based on those used in the Materials Project[9] to leverage on the large set of computed data available in that database.

Our calculated phase diagram predicts LGPS to be thermodynamically unstable at 0 K with respect to the following decomposition:

$$Li_{10}GeP_2S_{12} \rightarrow 2Li_3PS_4 + Li_4GeS_4 \quad (1)$$

The calculated Li_3PS_4 ground state is iso-structural with β-Li_3PO_4, consistent with the earlier findings of Holzwarth et al.[10] Nonetheless, the reaction energy for eq 1 is only −25 meV/atom, indicating that it can be easily stabilized by entropic effects or created as a metastable phase.

Using the methodology outlined in Ong et al.,[11] we plotted the lithium grand potential phase diagrams of the Li–Ge–P–S system at various lithium chemical potentials (μ_{Li}) of interest in Figure 1. Lithium grand potential phase diagrams represent the phase equilibria of a Li–Ge–P–S system that is open to lithium, which is relevant when the LGPS solid electrolyte is in contact with a reservoir of lithium, as is the case in a lithium battery. The voltage in a battery is the negative of the Li chemical potential. The Li chemical potentials in Figure 1 were chosen to elucidate the key changes in the equilibrium decomposition of LGPS as we go from the bulk metallic Li chemical potential (Figure 1a) to an environment where no Li-containing phases are present in the phase diagram (Figure 1c).

From Figure 1a, we may observe that, at the metallic lithium chemical potential, we predict that the LGPS solid electrolyte will consume lithium to decompose to a combination of Li_2S, Li_3P, and $Li_{15}Ge_4$. At -1.8 eV $< \mu_{Li} < -2.4$ eV (Figure 1b), LGPS decomposes via the equilibrium decomposition in eq 1. Finally, at even lower $\mu_{Li} > -2.4$ eV (Figure 1c), LGPS decomposes into P_2S_5, S, and GeS_2 with lithium extraction.

Received: November 4, 2011
Revised: December 8, 2011
Published: December 9, 2011

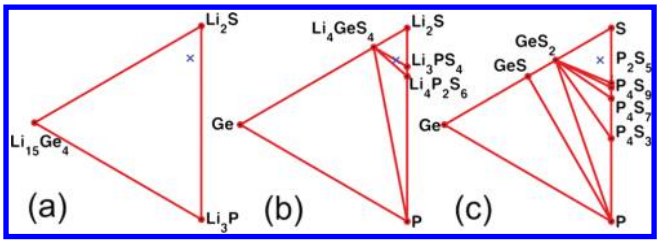

Figure 1. Phase evolution of the Li−Ge−P−S system as a function of Li chemical potential μ_{Li} at (a) 0 eV, (b) −1.8 eV, and (c) −2.5 eV. μ_{Li} = 0 eV corresponds to metallic Li. Labeled dots denote stable phases at each μ_{Li}. For all other compositions, the equilibrium state is formed by a combination of the stable phases in the triangle surrounding that composition. The LGPS composition is marked with a blue cross. For example, the equilibrium state of the LGPS composition is given by a combination of GeS_2, S, and P_2S_5 at μ_{Li} = −2.5 eV.

Though Kamaya et al.[3] reported that LGPS is stable for an electrochemical window in excess of 5 V vs Li/Li^+ with no observed electrolyte decomposition currents in that range, our calculations indicate that this material is unlikely to be stable against lithium. We propose that an alternative explanation for the wide electrochemical window of LGPS is that the decomposition of this material in contact with the electrodes results in the formation of either Li_2S (anode) or P_2S_5 (cathode), possibly in an amorphous form, which are components of the well-known glassy Li-ion conductors.[12] The formation of such a Li-conducting passivation layer would prevent further decomposition of the electrolyte with minimal impact on electrochemical performance. A similar solid electrolyte interphase (SEI) phenomenon has indeed been reported by Kobayashi et al.[13] for the similar $Li_{3.25}Ge_{0.25}P_{0.75}S_4$ thio-LISICON.

We also calculated the electrochemical window of LGPS on inert electrodes using the approach outlined by Ong et al.[14] Briefly, the approach involves the calculation of the density of states (DOS) of LGPS to determine the lowest unoccupied molecular orbital (LUMO) and highest occupied molecular orbital (HOMO) energies. Given the known limitations of GGA functionals in calculating band gaps, the DOS of LGPS was calculated using the Heyd−Scuseria−Erznerhof (HSE06) functional[15] and is given in Figure 2. We find that the HSE06

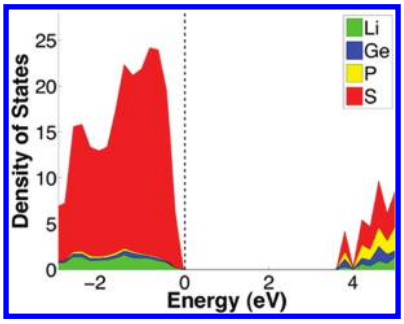

Figure 2. DOS of LGPS calculated with the HSE06 functional.

band gap is calculated to be around 3.6 eV, far smaller than the electrochemical window of >5 V reported by Kamaya et al. Because the electrochemical window estimated using this approach is an upper limit assuming inert electrodes, this result lends further credence to our hypothesis that the excellent electrochemical stability of LGPS is not due to the intrinsic stability of the material itself, but rather the result of passivation phenomenon.[13] We believe that the loss of Coulombic efficiency in the first cycles of the solid state battery constructed with LGPS[3] is evidence of lithium consumption, which creates the interfacial decomposition products.

To study the Li diffusion in LGPS, we performed ab initio molecular dynamics (MD) simulations under the Born−Oppenheimer approximation. The MD simulations were performed at elevated temperatures (600 K to 1500 K) to speed up diffusion and shorten the simulation time scale. The time step was chosen to be 2 fs, and the diffusion simulations were performed for 40 ps. No breaking of P−S or Ge−S bonds was observed during the simulations. More details about the simulations can be found in the Supporting Information.

The trajectories of Li diffusion during the ab inito MD simulations are shown in Figure 3. From our simulations, we

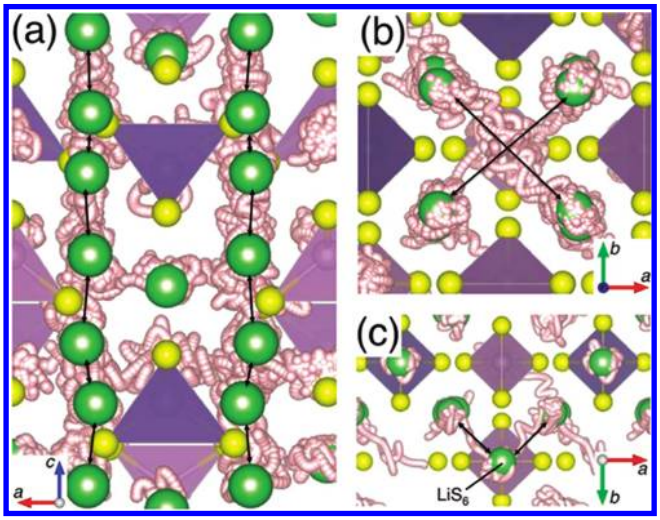

Figure 3. Trajectories (white) of Li atoms (Green) in ab initio MD simulations at 900 K. The 1D diffusion pathway along the *c* direction (a) and diffusion in the *ab* plane (b and c). PS_4 (GeS_4) tetrahedra in light (dark) purple. S atoms in yellow. The initial positions of nondiffusing atoms and all Li sites are shown for ease of visualization.

observe very facile Li diffusion in the 1D diffusion channels along the *c* direction (Figure 3a). This diffusion pathway is consistent with the hypothesis of Kamaya et al.[3] However, we also find significant Li hopping in the *ab* plane. Figure 3b shows one of these new diffusion pathways, which connect one LiS_4 tetrahedra to another LiS_4 tetrahedra in the diagonal directions in the *ab* plane. The diffusion in the *ab* plane is not surprising, because there is empty space for diffusion between the $(Ge_{0.5}P_{0.5})S_4$ tetrahedra and PS_4 tetrahedra (Figure 3a). Yet another diffusion pathway connects Li atoms in LiS_6 octahedra site to the *c*-axis diffusion channels (Figure 3c). This pathway in the *ab* plane connects the LiS_4 tetrahedra site to the LiS_6 octahedra site, which was originally regarded by Kamaya et al. as inactive for diffusion.

We calculated the diffusion coefficients for all pathways found by the MD simulations. The diffusion coefficient is calculated as the averaged mean square displacement of Li atoms over time. Convergence of diffusion coefficients is achieved with approximately 40 ps of MD simulations because of the relatively fast Li diffusion in this material. Figure 4 shows the Arrhenius plot for the various diffusion coefficients at temperatures from 600 K to 1500 K. From Figure 4a, we calculate an overall activation barrier of 0.21 eV for Li diffusion

dx.doi.org/10.1021/cm203303y | *Chem. Mater.* 2012, 24, 15−17

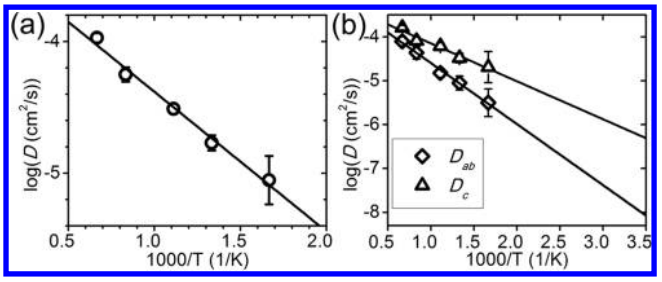

Figure 4. Arrhenius plot of (a) overall diffusion coefficient and the diffusion coefficient in the *c* direction D_c and in the *ab* plane D_{ab} (b). The error bar corresponds to statistical uncertainty in the fitting of the mean square displacement to time curve.

in LGPS. This calculated barrier is in remarkable agreement with the experimentally determined barrier of 0.24 eV,[3] despite the fact that the ab initio MD calculations were carried out at much higher temperatures than the experiments. The calculated diffusion extrapolates to a Li^+ conductivity of 9 mS/cm (with a range of 2 to 40 mS/cm) at 300 K, which again is in remarkable agreement with the experimental conductivity of 12 mS/cm.

From Figure 4b, we may observe that Li diffusion along the *c* direction is faster than the diffusion in the *ab* plane. We calculate activation barriers of 0.17 eV for the diffusivity in the *c* direction D_c and 0.28 eV for the diffusivity in the *ab* plane D_{ab}. Extrapolating from the Arrhenius plot, we find that D_c is predicted to be two orders of magnitude higher than D_{ab} at 300 K. The extrapolated conductivity at 300 K is around 40 mS/cm in the *c* direction and 0.9 mS/cm in the *ab* plane.

Our simulations show that LGPS is in fact a 3D ion conductor rather than a 1D ion conductor. The 3D diffusion network consists of 1D diffusion channels along the *c* direction and interchannel diffusion in the *ab* plane. This difference between 3D and 1D is significant as truly 1D conductors cannot retain their good conductivity in the macroscopic limit due the inevitable presence of channel blocking defects,[16] and some crossover between 1D channels is required to bypass such defects. The fact that the activation energy for the overall Li diffusivity is between the activation energy for the *c*-axis and *ab*-plane motion provides evidence that such crossovers are important for the overall transport. While diffusivity is predicted to be two orders of magnitude more facile in the *c* direction as compared to the *ab* directions at 300 K, there is nonetheless significant diffusion in the *ab* plane as well. The predicted conductivity in the *ab* plane at 300 K is as high as ~1 mS/cm, which is still comparable with state-of-the-art solid electrolytes.

In summary, we investigated the LGPS lithium super ionic conductor material using a variety of first principles techniques. We find that LGPS is a metastable phase in the calculated phase diagram. We also find that LGPS is not stable against reduction by lithium at low voltage or extraction of Li with decomposition at high voltage. Together with the calculated band gap of 3.6 eV, these predictions suggest that the observed electrochemical window greater than 5 V of this material is likely the result of a passivation phenomenon where either Li_2S or P_2S_5 is formed as a decomposition product.

Our ab initio MD simulations confirm fast Li diffusion in the 1D diffusion channel along the *c* direction but also predict two additional diffusion pathways in the *ab* plane. Though diffusion in the *ab* plane is not as facile as in the *c* direction, it nonetheless contributes to the overall performance of the material. Our calculated overall activation barrier and conductivity are in remarkable agreement with the experimental values.

■ ASSOCIATED CONTENT

Supporting Information

Computational details (PDF). This material is available free of charge via the Internet at http://pubs.acs.org.

■ AUTHOR INFORMATION

Corresponding Author

*E-mail: gceder@mit.edu.

■ ACKNOWLEDGMENTS

We would like to thank the Samsung Advanced Institute of Technology for their funding of this research. We also thank Lincoln Miara and Hyo Sug Lee for helpful discussions.

■ ABBREVIATIONS

LGPS, $Li_{10}GeP_2S_{12}$; MD, molecular dynamics; SEI, solid electrolyte interphase; GGA, generalized-gradient approximation; HSE06, Heyd−Scuseria−Ernzerhof; DOS, density of states

■ REFERENCES

(1) Armand, M.; Tarascon, J. M. *Nature* **2008**, *451* (7179), 652−657.
(2) Tarascon, J. M.; Armand, M. *Nature* **2001**, *414* (6861), 359−367.
(3) Kamaya, N.; Homma, K.; Yamakawa, Y.; Hirayama, M.; Kanno, R.; Yonemura, M.; Kamiyama, T.; Kato, Y.; Hama, S.; Kawamoto, K.; Mitsui, A. *Nat. Mater.* **2011**, *10* (9), 682−686.
(4) Kresse, G.; Furthmuller, J. *Phys. Rev. B* **1996**, *54* (16), 11169−11186.
(5) Blöchl, P. E. *Phys. Rev. B* **1994**, *50* (24), 17953−17979.
(6) Perdew, J. P.; Emzerhof, M.; Burke, K. *J. Chem. Phys.* **1996**, *105* (22), 9982−9985.
(7) Bergerhoff, G.; Hundt, R.; Sievers, R.; Brown, I. D. *J. Chem. Inf. Comput. Sci.* **1983**, *23* (2), 66−69.
(8) Ewald, P. P. *Ann. Phys.-Berlin* **1921**, *64* (3), 253−287.
(9) Jain, A.; Hautier, G.; Moore, C. J.; Ong, S. P.; Fischer, C. C.; Mueller, T.; Persson, K. A.; Ceder, G. *Comput. Mater. Sci.* **2011**, *50* (8), 2295−2310.
(10) Holzwarth, N. A. W.; Lepley, N. D.; Du, Y. A. *J. Power Sources* **2011**, *196* (16), 6870−6876.
(11) Ong, S. P.; Wang, L.; Kang, B.; Ceder, G. *Chem. Mater.* **2008**, *20* (5), 1798−1807.
(12) Murayama, M.; Sonoyama, N.; Yamada, A.; Kanno, R. *Solid State Ionics* **2004**, *170* (3−4), 173−180.
(13) Kobayashi, T.; Yamada, A.; Kanno, R. *Electrochim. Acta* **2008**, *53* (15), 5045−5050.
(14) Ong, S. P.; Andreussi, O.; Wu, Y.; Marzari, N.; Ceder, G. *Chem. Mater.* **2011**, *23* (11), 2979−2986.
(15) Heyd, J.; Scuseria, G. E.; Ernzerhof, M. *J. Chem. Phys.* **2003**, *118* (18), 8207−8215.
(16) Malik, R.; Burch, D.; Bazant, M.; Ceder, G. *Nano Lett.* **2010**, *10* (10), 4123−4127.